欠陥パイロクロア型 $Pb_2Ru_2O_{6.5}$ の構造

石澤伸夫[†]・ドボーレイダグラス[†]・須田勝美[‡]・赤澤亜美[¶]・勝又哲裕[¶]・稲熊宜之[¶]

[†] 名古屋工業大学セラミックス基盤工学研究センター　〒 507-0071 岐阜県多治見市旭ヶ丘 10-6-29

[‡] 東京工業大学応用セラミックス研究所　〒 226-8503 神奈川県横浜市緑区長津田町 4259

[¶] 学習院大学理学部化学科　〒 171-8588 東京都豊島区目白 1-5-1

Structure of Defect Pyrochlore-Type $Pb_2Ru_2O_{6.5}$

Nobuo Ishizawa[†], Douglas du Boulay[†], Katsumi Suda[‡], Tugumi Akazawa[¶], Tetsuhiro Katsumata[¶], and Yoshiyuki Inaguma[¶]

[†] Ceramics Research Laboratory, Nagoya Institute of Technology, Asahigaoka, Tajimi 507-0071, Japan

[‡] Materials and Structures Laboratory, Tokyo Institute of Technology, 4259 Nagatsuta Midori, Yokohama 226-8503

[¶] Department of Chemistry, Faculty of Science, Gakushuin University, 1-5-1 Mejiro, Toshima-ku, Tokyo 171-8588

Temperature dependence of the defect pyrochlore-type structure of $Pb_2Ru_2O_{6.5}$ has been investigated at 123, 193 and 293 K by the single-crystal diffraction method. The oxide anion vacancies order preferentially on one of two inversion centre related sites, thereby breaking the symmetry of the pyrochlore archetype. The Pb atoms are displaced by about 0.042 Å toward the oxide anion vacancy. The mean thermal expansion coefficient of the unit cell dimension was 11.8 x 10^{-6} in the investigated temperature region. The excess electrons of 6 eÅ^{-3} at the peak top are located about 0.8 Å along the principal axes from each Pb atom in the difference Fourier map, suggesting a disordered distortion of the Pb electron cloud.

[Received February 8, 2007; Accepted March 9, 2007]

1. Introduction

The pyrochlore $NaCa(Nb_2O_6)F$ adopts the space group symmetry $Fd\bar{3}m$, forming the archetype for a wide range of substitutionally related pyrochlore-like compounds with the general formula $A_2B_2O_6O'$ [1]. These materials also host a wide variety of technologically important physical properties. In particular, the fractionally populated $Pb_2Ru_2O_{6.5}$ pyrochlore-like ceramics of interest here, demonstrate high electrical conductivities, i.e., $2.3x10^{-4}$ Ω cm at 293 K [2] and find application as electrode materials and the conductive elements of thick film resistors [3].

The structure of $Pb_2O'_{0.5} \cdot Ru_2O_6$ was first reported by the neutron powder diffraction [4]. Hsu et al. [5] calculated the band structure of $Pb_2Ru_2O_{6.5}$ and suggested that the metallic behaviour of the compound is dominated by the admixture of partially-filled t_{2g} band of Ru 4d electrons and the Pb 6p band via the framework O atoms. They also pointed out that the Pb 6s band is about 10 eV deep from the Fermi level and unlikely to contribute to the metallic conduction as previously believed [6]. The present study was undertaken to investigate the temperature dependence of the $Pb_2Ru_2O_{6.5}$ structure.

2. Experimental

Crystals were grown from self-fluxing PbO and RuO_2 starting powders. They were mixed in 9:1 molar ratio (i. e., excess PbO) and placed in a platinum crucible. The temperature was raised from room temperature to 1523 K within 3 h, and maintained for 6 h before cooling at the rate of 5 K/h. Metallic black coloured crystals were grown to a maximum size of 9 x 7 x 4 mm^3. The oxygen content of the crystal was determined from the weight loss during the reduction of product at 773 K in a H_2 atmosphere by thermogravimetric analyzer. The Pb/Ru ratio was confirmed by the ICP analysis. The chemical composition of the crystals was $Pb_2Ru_2O_{6+x}$ where x=0.50±0.02. The electric and magnetic properties of the grown crystals have already been reported [2].

The sample has an irregular block in shape with

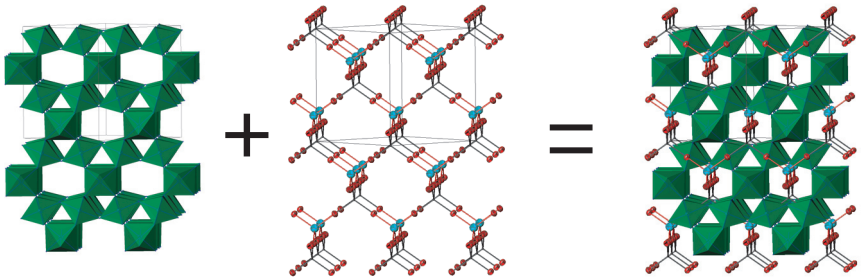

Fig. 1. Interpenetrating sublattices of B_2O_6 (left) and the A_2O' sublattice (centre) results in the $A_2B_2O_7$ pyrochlore structure (right). The B_2O_6 sublattice is composed of corner-sharing BO_6 octahedra. The O' atoms are further divided into O3 and V_o (vacancy presented as a point) to describe $Pb_2Ru_2O_{6.5}$. The 293 K parameters are used for the illustration with thermal ellipsoids drawn at the 99% probability level. The unit cell is given by the solid line.

100x120x133 μm^3. X-ray diffraction data were measured on a Rigaku RAPID imaging plate diffractometer [7] using Mo Kα radiation with the Oxford cryosystems liquid nitrogen air stream at 123, 193 and 293 K. At Mo radiation wavelengths, the dominant scatterer, Pb, displays very strong anomalous dispersion. Satisfactory refinement results were only obtained after refining the absolute structure from separately averaged Friedel pairs. Presumably because the Pb displacement was the dominant contributor of density to the inversion symmetry breaking, enantiomeric sensitivity of the absolute structure refinement was enhanced. The extinction correction also played a dominant role in the refinement [8]. Attenuation factors of around 50% were observed for the strongest reflections, well outside the kinematic approximation and suggesting the associated correction factors are highly questionable. The Flack parameter provides quite convincing evidence that the sample studied was monodomain. Crystal data at 123 K are given in Table 1.

3. Results and discussion

Results of refinements are given in Table 2. The structural parameters at 123, 193 and 293 K are given in Table 3. Selected interatomic distances and bond angles are given in Table 4. The ideal pyrochlore structure is easier to discuss in terms of its two distinct, interpenetrating sublattices represented as $A_2O' \cdot B_2O_6$ and shown more succinctly in Fig. 1. Each B site is octahedrally coordinated to six O atoms and collectively they form a semi-infinite three-dimensional network of six-membered, corner sharing octahedral ring systems. On the other hand, the A_2O' sublattice adopts the cuprite-like structure (Cu_2O) shown in Fig. 1 (middle), filling the voids and cavities formed by the hexagonal rings of linked octahedra. Each A site is linearly coordinated by two O' sites and each O' site is tetrahedrally coordinated to four A sites.

When the A sites of the pyrochlore archetype are filled with Tl^+, Pb^{2+} or Bi^{3+}, having polarizable $6s^2$ lone pair electrons, the population of the O' sites becomes variable and the stoichiometry is better written as $A_2O'x.B_2O_6$, with x in the range between 0 and 1. In the case of $Pb_2O'_{0.5}.Ru_2O_6$, our focus here, defect ordering destroys the A site inversion centres of the $Fd\bar{3}m$ archetype, leading to the noncentrosymmetric subgroup $F\bar{4}3m$ with two symmetry distinct O' sites, i.e., O3 and V_o.

The linked $Pb_4V_o \cdot Pb_4O3$ clusters are shown in Fig. 2. Because of the asymmetry of the O3–Pb–V_o vacancy ordering in ideally defect-ordered $Pb_2Ru_2O_{6.5}$, the Pb

Table 1. Crystal data at 123 K

Compound	$Pb_2Ru_2O_{6.5}$
Crystal system:	Cubic
Space group	$F\bar{4}3m$
a	10.241 (2) Å
V	1074.1 (6) $Å^3$
Z	8
Dx	8.912 Mg m^{-3}
Mr	720.54
Radiation	Mo K α radiation

Table 2. Results of refinements. N1: Number of measured reflections. N2: Number of reflections used for refinements. Rint: Merge R factor for N1. R: Final R factor for N2.

T(K)	*a*	N1	Rint	θ max	N2	R
123	10.241 (2)	10286	0.088	45.26	503	0.035
193	10.253 (2)	11080	0.081	45.26	510	0.033
293	10.262 (2)	10663	0.034	45.21	506	0.040

Table 3. Fractional coordinates and atomic displacement parameters ($Å^2$) at 123, 193 and 293 K.

Atom	T(K)	x	y	z	Uiso	U11	U22	U33	U12	U13	U23
Pb	123	.87738(10)	.87738(10)	.87738(10)	.0047(3)	.0047(3)	.0047(3)	.0047(3)	-.00067(17)	-.00067(17)	-.00067(17)
	193	.87756(6)	.87756(6)	.87756(6)	.0078(3)	.0078(3)	.0078(3)	.0078(3)	-.00144(15)	-.00144(15)	-.00144(15)
	293	.87733(6)	.87733(6)	.87733(6)	.0117(2)	.0117(2)	.0117(2)	.0117(2)	-.00120(13)	-.00120(13)	-.00120(13)
Ru	123	.3752(2)	.3752(2)	.3752(2)	.0035(5)	.0035(5)	.0035(5)	.0035(5)	-.0002(3)	-.0002(3)	-.0002(3)
	193	.37468(12)	.37468(12)	.37468(12)	.0042(4)	.0042(4)	.0042(4)	.0042(4)	.0002(2)	.0002(2)	.0002(2)
	293	.37518(10)	.37518(10)	.37518(10)	.0074(4)	.0074(4)	.0074(4)	.0074(4)	-.00049(19)	-.00049(19)	-.00049(19)
O1	123	.3025(11)	0	0	.006(2)	.010(4)	.0041(18)	.0041(18)	0	0	.001(3)
	193	.3022(8)	0	0	.006(2)	.008(3)	.0053(15)	.0053(15)	0	0	-.000(2)
	293	.3023(9)	0	0	.012(2)	.014(3)	.0107(17)	.0107(17)	0	0	-.002(2)
O2	123	.4497(9)	0.25	0.25	.004(2)	.005(3)	.0038(18)	.0038(18)	0	0	-.003(3)
	193	.4497(8)	0.25	0.25	.007(2)	.004(3)	.0079(17)	.0079(17)	0	0	-.001(2)
	293	.4500(8)	0.25	0.25	.010(2)	.010(3)	.0097(16)	.0097(16)	0	0	-.002(2)
O3	123	0.75	0.75	0.75	.006(4)	.006(4)	.006(4)	.006(4)	0	0	0
	193	0.75	0.75	0.75	.006(3)	.006(3)	.006(3)	.006(3)	0	0	0
	293	0.75	0.75	0.75	.013(3)	.013(3)	.013(3)	.013(3)	0	0	0

inversion symmetry of the archetype is broken. That permits the Pb–Pb contacts around the perimeter of the Pb_4V_o cluster to contract around the vacancy, reducing to 3.561(1) Å in length while the Pb–Pb contacts defining the Pb_4O_3 cluster expand to 3.696(1) Å. There is a concomitant increase in the Pb–O3 bond length to 2.2631(6) Å, whereas the Pb–V_o distance decreases to 2.1804(6) Å. The metallic Pb crystal with the 4.9496(3) Å fcc cell leads to twelve metallic Pb--Pb bonds 3.50 Å in length [9], which is close to the Pb--Pb distance of the Pb_4V_o cluster.

There is a small but perceptible systematic increases in the cubic cell dimensions with increasing temperature. The mean thermal expansion coefficient of the cell dimension is 11.8 x 10^{-6} in the investigated temperature region. Temperature dependent changes in the fractional atomic coordinates were small.

The vibrational motion of Ru is relatively small, in keeping with its three short and strong octahedral bonds to each of O1 and O2. Those bonds differ in length by only 0.012(3) Å at 293 K so despite permissive symmetry, the Ru atom is scarcely displaced from the geometric centre of the RuO_6 octahedron.

The isotropic atomic displacement parameters are plotted in Fig. 3 as a function of temperature. Taking into consideration their estimated standard uncertainties, the Uiso values generally change almost proportional to tem-

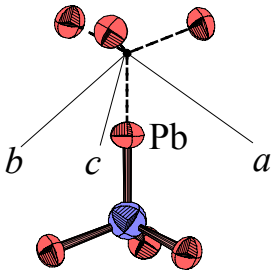

Fig. 2. Pb_4O3 and Pb_4V clusters at 193K with ellipsoids drawn at the 99% probability level. The oxygen vacancy (V_o) is located at the origin of the unit cell.

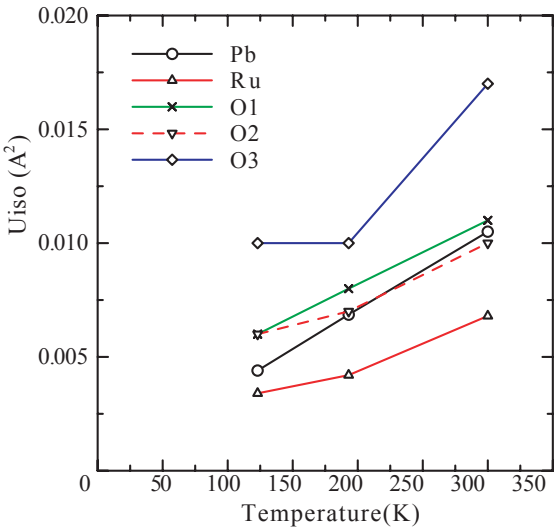

Fig. 3. Changes of isotropic atomic displacement parameters with temperature.

Table 4. Selected interatomic distances (Å) and angles (°).

	123K	193K	293K
Pb—O3	2.2595(10)	2.2652(7)	2.2631(6)
Pb—$O2^{i}$	2.557(7)	2.559(6)	2.560(6)
Pb—$O1^{ii}$	2.559(8)	2.561(5)	2.563(6)
Ru—$O1^{iii}$	1.955(5)	1.963(3)	1.960(3)
Ru—$O2^{iv}$	1.967(4)	1.965(3)	1.972(3)
Ru^{v}—O1—Ru^{vi}	135.3(6)	135.5(4)	135.1(5)
Ru^{v}—O2—Ru	134.3(5)	133.9(4)	134.2(4)

Symmetry codes: (i) 1/2+ y, 1 − z, 3/2 − x; (ii) 1 + y, 1 − z, 1 − x; (iii) 1/2+ y, 1/2+ z, x; (iv) y, z, x; (v) x, 1/2 − y, 1/2 − z; (vi) x, y − 1/2, z − 1/2

perature except for O3. The odd behaviour of O3 may suggest a possible structural change at low temperatures.

Because of the potential, and numerous, metal-metal bonds involved in this material, bond valence sums (BVSs) derived and applicable only to fully ionic compounds, are necessarily of dubious character. Charge neutrality of the $Pb_2Ru_2O_{6.5}$ stoichiometry favours a mean valence of +4.5 for Ru in addition to the formal ionic charges of +2, -2 for Pb and O respectively. BVS values at 293 K were 2.42 for Pb, 4.62 for Ru, -2.16 for O1, -2.10 for O2 and -2.64 for O3. Large deviations for Pb and O3 from the formal values may suggest a possible polarization of the Pb electron cloud, which can be schematically modeled as an electric dipole composed of Pb^{4+} and the $6s^2$ lone pair electrons with the former oriented toward O3. The maximum difference electron density of about 6 $eÅ^{-3}$ was located about 0.8 Å along the principal axes from each Pb atom in the 123 K difference Fourier map. The height and location of the peak was almost the same at 193 and 293 K. The peak may evidence a disordered distortion of the Pb electron cloud originating in the $6s^2$ electrons.

An excess electron density maximizing at 4 $eÅ^{-3}$ was found at the V_o position at 123 K. The peak height decreased to 2 $eÅ^{-3}$ at 193 K and disappeared at 293 K. Although the refinements assuming oxygen atom disorder between O3 and V_o sites were undertaken at 123 K, no significant improvement of R factors were obtained. A detailed study with more accurate data could reveal the partial O atom disorder between O3 and V_o.

Acknowledgement

This study was supported by grants-in-aid for Scientific Research No. 18206071 and High-Technology Research Center Project from the Ministry of Education, Culture, Sports, Science and Technology, Japan.

Reference

1) H. R. Gaertner, *Neues Jahrbuch FUER Mineralogie, Geologie und Palaeontologie. Beilagen, Abt. A,* 1930, **61**, 1-30.
2) T. Akazawa, Y. Inaguma, T. Katsumata, K. Hiraki, T. Takahashi, *J. Crystal Growth*, 2004, **271**[3-4], 445-449.
3) P. F. Carcia, A. Ferretti, A. Suna, *J. Appl. Phys.* 1982, **53**, 5282-5288.
4) R. A Beyerlein, H. S. Horowitz, J. M. Longo, M. E. Leonowicz, J. D. Jorgensen, F. J. Rotella, *J. Sollid State Chem.* 1984, **51**, 253-265.
5) W. Y. Hsu, R. V. Kasowski, T. Miller, T.-C. Chiang, *Appl. Phys. Lett.* 1988, **2**[10] 792-794.
6) J. M. Longo, P. M. Raccah, J. B. Goodenough, *Mater. Res. Bull.*, 1969, **4**, 191-202.
7) Rapid Auto. Manual No. MJ13159A01, 1999, Rigaku Corporation, Tokyo, Japan
8) S. R. Hall, D. du Boulay, R. Olthof-Hazekamp, Eds. Xtal3.7 System. http://Xtal.sourceforge.net/. 2000.
9) E. A.Owen, E. L. Yates, *Philosophical Magazine*, 1933, **15**, 472-488.